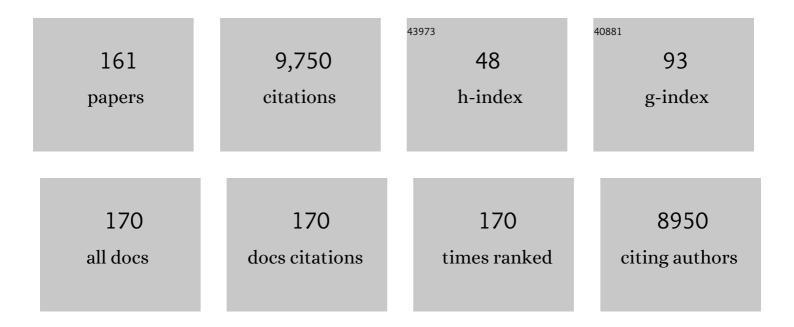
Lars-Oliver Essen

List of Publications by Year in descending order

Source: https://exaly.com/author-pdf/9227051/publications.pdf Version: 2024-02-01



#	Article	IF	CITATIONS
1	Inactive pseudoenzyme subunits in heterotetrameric BbsCD, a novel shortâ€chain alcohol dehydrogenase involved in anaerobic toluene degradation. FEBS Journal, 2022, 289, 1023-1042.	2.2	2
2	Structure of the Yeast Cell Wall Integrity Sensor Wsc1 Reveals an Essential Role of Surface-Exposed Aromatic Clusters. Journal of Fungi (Basel, Switzerland), 2022, 8, 379.	1.5	6
3	Serial crystallography captures dynamic control of sequential electron and proton transfer events in a flavoenzyme. Nature Chemistry, 2022, 14, 677-685.	6.6	24
4	Bistable Photoswitch Allows in Vivo Control of Hematopoiesis. ACS Central Science, 2022, 8, 57-66.	5.3	18
5	Lightâ€induced fermenter production of derivatives of the sweet protein monellin is maximized in prestationary <i>Saccharomyces cerevisiae</i> cultures. Biotechnology Journal, 2022, 17, e2100676.	1.8	3
6	Ultrafast photoreduction dynamics of a new class of CPD photolyases. Photochemical and Photobiological Sciences, 2021, 20, 733-746.	1.6	2
7	The archaeal triphosphate tunnel metalloenzyme SaTTM defines structural determinants for the diverse activities in the CYTH protein family. Journal of Biological Chemistry, 2021, 297, 100820.	1.6	10
8	Conformational Change of Tetratricopeptide Repeats Region Triggers Activation of Phytochrome-Associated Protein Phosphatase 5. Frontiers in Plant Science, 2021, 12, 733069.	1.7	1
9	Ultrafast Photoconversion Dynamics of the Knotless Phytochrome SynCph2. International Journal of Molecular Sciences, 2021, 22, 10690.	1.8	5
10	An Optogenetic Toolbox for Synergistic Regulation of Protein Abundance. ACS Synthetic Biology, 2021, 10, 3411-3421.	1.9	4
11	A novel class of Candida glabrata cell wall proteins with β-helix fold mediates adhesion in clinical isolates. PLoS Pathogens, 2021, 17, e1009980.	2.1	9
12	Functional reprogramming of Candida glabrata epithelial adhesins: the role of conserved and variable structural motifs in ligand binding. Journal of Biological Chemistry, 2020, 295, 12512-12524.	1.6	8
13	Structural base for the transfer of GPI-anchored glycoproteins into fungal cell walls. Proceedings of the National Academy of Sciences of the United States of America, 2020, 117, 22061-22067.	3.3	21
14	The Phosphatase PP2A Interacts With ArnA and ArnB to Regulate the Oligomeric State and the Stability of the ArnA/B Complex. Frontiers in Microbiology, 2020, 11, 1849.	1.5	15
15	Electron transfer and spin dynamics of the radical-pair in the cryptochrome from <i>Chlamydomonas reinhardtii</i> by computational analysis. Journal of Chemical Physics, 2020, 152, 065101.	1.2	13
16	An Optogenetic Tool for Induced Protein Stabilization Based on the Phaeodactylum tricornutum Aureochrome 1a Light–Oxygen–Voltage Domain. Journal of Molecular Biology, 2020, 432, 1880-1900.	2.0	22
17	A topologically distinct class of photolyases specific for UV lesions within single-stranded DNA. Nucleic Acids Research, 2020, 48, 12845-12857.	6.5	9
18	Diversity of GPI-anchored fungal adhesins. Biological Chemistry, 2020, 401, 1389-1405.	1.2	17

#	Article	IF	CITATIONS
19	Kin discrimination in social yeast is mediated by cell surface receptors of the Flo11 adhesin family. ELife, 2020, 9, .	2.8	30
20	Structural and Functional Characterization of an Electron Transfer Flavoprotein Involved in Toluene Degradation in Strictly Anaerobic Bacteria. Journal of Bacteriology, 2019, 201, .	1.0	15
21	Ultrafast Oxidation of a Tyrosine by Proton-Coupled Electron Transfer Promotes Light Activation of an Animal-like Cryptochrome. Journal of the American Chemical Society, 2019, 141, 13394-13409.	6.6	37
22	Structural changes within the bifunctional cryptochrome/photolyase CraCRY upon blue light excitation. Scientific Reports, 2019, 9, 9896.	1.6	17
23	Structure and interactions of the archaeal motility repression module ArnA–ArnB that modulates archaellum gene expression in Sulfolobus acidocaldarius. Journal of Biological Chemistry, 2019, 294, 7460-7471.	1.6	26
24	Modulating Protein–Protein Interactions with Visibleâ€Lightâ€Responsive Peptide Backbone Photoswitches. ChemBioChem, 2019, 20, 1417-1429.	1.3	33
25	Optogenetic Downregulation of Protein Levels with an Ultrasensitive Switch. ACS Synthetic Biology, 2019, 8, 1026-1036.	1.9	24
26	The Glycosylphosphatidylinositol-Anchored <i>DFG</i> Family Is Essential for the Insertion of Galactomannan into the β-(1,3)-Glucan–Chitin Core of the Cell Wall of Aspergillus fumigatus. MSphere, 2019, 4, .	1.3	28
27	Deconstructing and repurposing the light-regulated interplay between Arabidopsis phytochromes and interacting factors. Communications Biology, 2019, 2, 448.	2.0	22
28	Comparative biochemical and structural analysis of the flavin-binding dodecins from Streptomyces davaonensis and Streptomyces coelicolor reveals striking differences with regard to multimerization. Microbiology (United Kingdom), 2019, 165, 1095-1106.	0.7	4
29	Nicotinamide Adenine Dinucleotides Arrest Photoreduction of Class II DNA Photolyases in FADH Ë™ State. Photochemistry and Photobiology, 2018, 94, 81-87.	1.3	7
30	Sub-nanosecond tryptophan radical deprotonation mediated by a protein-bound water cluster in class II DNA photolyases. Chemical Science, 2018, 9, 1200-1212.	3.7	30
31	Delocalized hole transport coupled to sub-ns tryptophanyl deprotonation promotes photoreduction of class II photolyases. Physical Chemistry Chemical Physics, 2018, 20, 25446-25457.	1.3	9
32	Structural and Functional Characterization of PA14/Flo5-Like Adhesins From Komagataella pastoris. Frontiers in Microbiology, 2018, 9, 2581.	1.5	6
33	Arabidopsis phytochrome A nuclear translocation is mediated by a farâ€red elongated hypocotyl 1–importin complex. Plant Journal, 2018, 96, 1255-1268.	2.8	25
34	Crystal structure of an Lrs14-like archaeal biofilm regulator from <i>Sulfolobus acidocaldarius</i> . Acta Crystallographica Section D: Structural Biology, 2018, 74, 1105-1114.	1.1	4
35	Light-Driven Domain Mechanics of a Minimal Phytochrome Photosensory Module Studied by EPR. Structure, 2018, 26, 1534-1545.e4.	1.6	23
36	A light-triggered transmembrane porin. Chemical Communications, 2018, 54, 9623-9626.	2.2	9

#	Article	IF	CITATIONS
37	Structure of the bifunctional cryptochrome aCRY from Chlamydomonas reinhardtii. Nucleic Acids Research, 2018, 46, 8010-8022.	6.5	51
38	Twist and turn: a revised structural view on the unpaired bubble of class II CPD photolyase in complex with damaged DNA. IUCrJ, 2018, 5, 608-618.	1.0	7
39	Wing phosphorylation is a major functional determinant of the Lrs14â€ŧype biofilm and motility regulator AbfR1 in <i>Sulfolobus acidocaldarius</i> . Molecular Microbiology, 2017, 105, 777-793.	1.2	32
40	Hyperactivity of the Arabidopsis cryptochrome (cry1) L407F mutant is caused by a structural alteration close to the cry1 ATP-binding site. Journal of Biological Chemistry, 2017, 292, 12906-12920.	1.6	5
41	Structural communication between the chromophoreâ€binding pocket and the Nâ€ŧerminal extension in plant phytochrome phyB. FEBS Letters, 2017, 591, 1258-1265.	1.3	7
42	Divalent Cations Increase DNA Repair Activities of Bacterial (6â€4) Photolyases. Photochemistry and Photobiology, 2017, 93, 323-330.	1.3	8
43	Analysis of c-di-GMP Levels Synthesized by a Photoreceptor Protein in Response to Different Light Qualities Using an In Vitro Enzymatic Assay. Methods in Molecular Biology, 2017, 1657, 187-204.	0.4	1
44	Structural and evolutionary aspects of algal blue light receptors of the cryptochrome and aureochrome type. Journal of Plant Physiology, 2017, 217, 27-37.	1.6	22
45	EHB1 and AGD12, two calcium-dependent proteins affect gravitropism antagonistically in Arabidopsis thaliana. Journal of Plant Physiology, 2016, 206, 114-124.	1.6	17
46	Extended Electron-Transfer in Animal Cryptochromes Mediated by a Tetrad of Aromatic Amino Acids. Biophysical Journal, 2016, 111, 301-311.	0.2	77
47	<i>Rhodobacter sphaeroides</i> CryB is a bacterial cryptochrome with (6–4) photolyase activity. FEBS Journal, 2016, 283, 4291-4309.	2.2	20
48	Mapping light-driven conformational changes within the photosensory module of plant phytochrome B. Scientific Reports, 2016, 6, 34366.	1.6	28
49	Allosteric communication between DNA-binding and light-responsive domains of diatom class I aureochromes. Nucleic Acids Research, 2016, 44, 5957-5970.	6.5	53
50	Essential Role of an Unusually Long-lived Tyrosyl Radical in the Response to Red Light of the Animal-like Cryptochrome aCRY. Journal of Biological Chemistry, 2016, 291, 14062-14071.	1.6	51
51	Structure of a Native-like Aureochrome 1a LOV Domain Dimer from Phaeodactylum tricornutum. Structure, 2016, 24, 171-178.	1.6	47
52	Cyclic mononucleotide- and Clr-dependent gene regulation in Sinorhizobium meliloti. Microbiology (United Kingdom), 2016, 162, 1840-1856.	0.7	21
53	Conformational heterogeneity of the Pfr chromophore in plant and cyanobacterial phytochromes. Frontiers in Molecular Biosciences, 2015, 2, 37.	1.6	26
54	Interactions by the Fungal Flo11 Adhesin Depend on a Fibronectin Type III-like Adhesin Domain Girdled by Aromatic Bands. Structure, 2015, 23, 1005-1017.	1.6	51

#	Article	IF	CITATIONS
55	The family of phytochrome-like photoreceptors: diverse, complex and multi-colored, but very useful. Current Opinion in Structural Biology, 2015, 35, 7-16.	2.6	102
56	Structural Hot Spots Determine Functional Diversity of the Candida glabrata Epithelial Adhesin Family. Journal of Biological Chemistry, 2015, 290, 19597-19613.	1.6	38
57	Phototransformation of the Red Light Sensor Cyanobacterial Phytochrome 2 from Synechocystis Species Depends on Its Tongue Motifs. Journal of Biological Chemistry, 2014, 289, 25590-25600.	1.6	19
58	Structure of the epimerization domain of tyrocidine synthetase A. Acta Crystallographica Section D: Biological Crystallography, 2014, 70, 1442-1452.	2.5	45
59	Tyrosine 263 in Cyanobacterial Phytochrome <scp>C</scp> ph1 Optimizes Photochemistry at the prelumiâ€ <scp>R</scp> →lumiâ€R Step. Photochemistry and Photobiology, 2014, 90, 786-795.	1.3	13
60	Cellular Metabolites Enhance the Light Sensitivity of <i>Arabidopsis</i> Cryptochrome through Alternate Electron Transfer Pathways Â. Plant Cell, 2014, 26, 4519-4531.	3.1	58
61	Photo-sensitive degron variants for tuning protein stability by light. BMC Systems Biology, 2014, 8, 128.	3.0	56
62	Voltage-dependent anion channels: the wizard of the mitochondrial outer membrane. Biological Chemistry, 2014, 395, 1435-1442.	1.2	39
63	Structure-Based Engineering of a Minimal Porin Reveals Loop-Independent Channel Closure. Biochemistry, 2014, 53, 4826-4838.	1.2	26
64	Structural and Evolutionary Aspects of Antenna Chromophore Usage by Class II Photolyases. Journal of Biological Chemistry, 2014, 289, 19659-19669.	1.6	39
65	A LOV2 Domain-Based Optogenetic Tool to Control Protein Degradation and Cellular Function. Chemistry and Biology, 2013, 20, 619-626.	6.2	227
66	Structure of the Cyanobacterial Phytochrome 2 Photosensor Implies a Tryptophan Switch for Phytochrome Signaling. Journal of Biological Chemistry, 2013, 288, 35714-35725.	1.6	80
67	Structural basis for promiscuity and specificity during <i>Candida glabrata</i> invasion of host epithelia. Proceedings of the National Academy of Sciences of the United States of America, 2012, 109, 16864-16869.	3.3	64
68	Bioactive cyclometalated phthalimides: design, synthesis and kinase inhibition. Dalton Transactions, 2012, 41, 9337.	1.6	27
69	Localized Dimerization and Nucleoid Binding Drive Gradient Formation by the Bacterial Cell Division Inhibitor MipZ. Molecular Cell, 2012, 46, 245-259.	4.5	105
70	Complex Gadolinium–Oxo Clusters Formed along Concave Protein Surfaces. ChemBioChem, 2012, 13, 2187-2190.	1.3	3
71	Flexibility of the N-Terminal mVDAC1 Segment Controls the Channel's Gating Behavior. PLoS ONE, 2012, 7, e47938.	1.1	46
72	Solid-State NMR Spectroscopic Study of Chromophore–Protein Interactions in the Pr Ground State of Plant Phytochrome A. Molecular Plant, 2012, 5, 698-715.	3.9	30

#	Article	IF	CITATIONS
73	CryB from <i>Rhodobacter sphaeroides</i> : a unique class of cryptochromes with new cofactors. EMBO Reports, 2012, 13, 223-229.	2.0	82
74	Lightâ€induced alteration of câ€diâ€CMP level controls motility of <i>Synechocystis</i> sp. PCC 6803. Molecular Microbiology, 2012, 85, 239-251.	1.2	103
75	Chemical engineering of Mycobacterium tuberculosis dodecin hybrids. Chemical Communications, 2011, 47, 11071.	2.2	6
76	On the Structure and Dynamics of Duplex GNA. Journal of Organic Chemistry, 2011, 76, 7964-7974.	1.7	22
77	Signaling Kinetics of Cyanobacterial Phytochrome Cph1, a Light Regulated Histidine Kinase. Biochemistry, 2011, 50, 6178-6188.	1.2	19
78	Structurally Sophisticated Octahedral Metal Complexes as Highly Selective Protein Kinase Inhibitors. Journal of the American Chemical Society, 2011, 133, 5976-5986.	6.6	218
79	Structure of the Chromophore Binding Pocket in the Pr State of Plant Phytochrome phyA. Journal of Physical Chemistry B, 2011, 115, 1220-1231.	1.2	38
80	Spectroscopy and a High-Resolution Crystal Structure of Tyr263 Mutants of Cyanobacterial Phytochrome Cph1. Journal of Molecular Biology, 2011, 413, 115-127.	2.0	71
81	Spectroscopic and Photochemical Characterization of the Redâ€Light Sensitive Photosensory Module of Cph2 from <i>Synechocystis</i> PCC 6803. Photochemistry and Photobiology, 2011, 87, 160-173.	1.3	41
82	Lightâ€generated Paramagnetic Intermediates in BLUF Domains ^{â€} . Photochemistry and Photobiology, 2011, 87, 574-583.	1.3	12
83	The Cryptochromes: Blue Light Photoreceptors in Plants and Animals. Annual Review of Plant Biology, 2011, 62, 335-364.	8.6	723
84	Strategies and Perspectives in Ionâ€Channel Engineering. ChemBioChem, 2011, 12, 830-839.	1.3	20
85	Crystal structures of an archaeal class II DNA photolyase and its complex with UV-damaged duplex DNA. EMBO Journal, 2011, 30, 4437-4449.	3.5	82
86	The Electronic State of Flavoproteins: Investigations with Proton Electron–Nuclear Double Resonance. Applied Magnetic Resonance, 2010, 37, 339-352.	0.6	26
87	Structural and functional characterization of a synthetically modified OmpG. Bioorganic and Medicinal Chemistry, 2010, 18, 7716-7723.	1.4	9
88	Structural basis of flocculin-mediated social behavior in yeast. Proceedings of the National Academy of Sciences of the United States of America, 2010, 107, 22511-22516.	3.3	113
89	Structural characterization of a Â-turn mimic within a protein-protein interface. Proceedings of the National Academy of Sciences of the United States of America, 2010, 107, 18336-18341.	3.3	42
90	Atomic resolution duplex structure of the simplified nucleic acidGNA. Chemical Communications, 2010, 46, 1094-1096.	2.2	35

#	Article	IF	CITATIONS
91	An Asymmetric Model for Na+-translocating Glutaconyl-CoA Decarboxylases. Journal of Biological Chemistry, 2009, 284, 28401-28409.	1.6	12
92	Photoreduction of the Folate Cofactor in Members of the Photolyase Family. Journal of Biological Chemistry, 2009, 284, 21670-21683.	1.6	25
93	αâ€Helical Cytolysins: Molecular Tunnelâ€Boring Machines in Action. ChemBioChem, 2009, 10, 2305-2307.	1.3	2
94	On the Function and Structure of Synthetically Modified Porins. Angewandte Chemie - International Edition, 2009, 48, 4853-4857.	7.2	21
95	Structural Basis and Stereochemistry of Triscatecholate Siderophore Binding by FeuA. Angewandte Chemie - International Edition, 2009, 48, 7924-7927.	7.2	51
96	Cover Picture: On the Function and Structure of Synthetically Modified Porins (Angew. Chem. Int. Ed.) Tj ETQqO	0	Overlock 10 1
97	Dwelling in the dark: procedures for the crystallography of phytochromes and other photochromic proteins. Acta Crystallographica Section D: Biological Crystallography, 2009, 65, 1232-1235.	2.5	6
98	The sodiumâ€dependent <scp>d</scp> â€glucose transport protein of <i>Helicobacter pylori</i> . Molecular Microbiology, 2009, 71, 391-403.	1.2	28
99	Structural basis for the <i>erythro</i> â€stereospecificity of the <scp>l</scp> â€arginine oxygenase VioC in viomycin biosynthesis. FEBS Journal, 2009, 276, 3669-3682.	2.2	64
100	Priorities in emergency obstetric care in Bolivia––maternal mortality and nearâ€miss morbidity in metropolitan La Paz. BJOG: an International Journal of Obstetrics and Gynaecology, 2009, 116, 1210-1217.	1.1	43
101	Photocycle dynamics of the E149A mutant of cryptochrome 3 from Arabidopsis thaliana. Journal of Photochemistry and Photobiology B: Biology, 2009, 97, 94-108.	1.7	13
102	Structural and functional analysis of the gpsA gene product of Archaeoglobus fulgidus: A glycerol-3-phosphate dehydrogenase with an unusual NADP+ preference. Protein Science, 2009, 13, 3161-3171.	3.1	9
103	AcrB et al.: Obstinate contaminants in a picogram scale. One more bottleneck in the membrane protein structure pipeline. Journal of Structural Biology, 2009, 166, 107-111.	1.3	22
104	Chromophore Structure of Cyanobacterial Phytochrome Cph1 in the Pr State: Reconciling Structural and Spectroscopic Data by QM/MM Calculations. Biophysical Journal, 2009, 96, 4153-4163.	0.2	66
105	Chapter 13 Nonribosomal Peptide Synthetases. Methods in Enzymology, 2009, 458, 337-351.	0.4	73
106	Nonâ€Heme Hydroxylase Engineering For Simple Enzymatic Synthesis of <scp>L</scp> â€ <i>threo</i> â€Hydroxyaspartic Acid. ChemBioChem, 2008, 9, 374-376.	1.3	24
107	Influence of a Joining Helix on the BLUF Domain of the YcgF Photoreceptor from <i>Escherichia coli</i> . ChemBioChem, 2008, 9, 2463-2473.	1.3	25
108	Duplex Structure of a Minimal Nucleic Acid. Journal of the American Chemical Society, 2008, 130, 8158-8159.	6.6	116

#	Article	IF	CITATIONS
109	Structural and Kinetic Properties of a β-Hydroxyacid Dehydrogenase Involved in Nicotinate Fermentation. Journal of Molecular Biology, 2008, 382, 802-811.	2.0	11
110	The Crystal Structure of Enamidase: A Bifunctional Enzyme of the Nicotinate Catabolism. Journal of Molecular Biology, 2008, 384, 837-847.	2.0	7
111	Ion-channel engineering. Annual Reports on the Progress of Chemistry Section C, 2008, 104, 165.	4.4	4
112	How to tailor non-ribosomal peptide products—new clues about the structures and mechanisms of modifying enzymes. Molecular BioSystems, 2008, 4, 387.	2.9	36
113	The structure of a complete phytochrome sensory module in the Pr ground state. Proceedings of the National Academy of Sciences of the United States of America, 2008, 105, 14709-14714.	3.3	359
114	Crystal Structure of the Termination Module of a Nonribosomal Peptide Synthetase. Science, 2008, 321, 659-663.	6.0	311
115	Recognition and repair of UV lesions in loop structures of duplex DNA by DASH-type cryptochrome. Proceedings of the National Academy of Sciences of the United States of America, 2008, 105, 21023-21027.	3.3	147
116	Light-induced chromophore activity and signal transduction in phytochromes observed by ¹³ C and ¹⁵ N magic-angle spinning NMR. Proceedings of the National Academy of Sciences of the United States of America, 2008, 105, 15229-15234.	3.3	85
117	The Dodecin from Thermus thermophilus, a Bifunctional Cofactor Storage Protein. Journal of Biological Chemistry, 2007, 282, 33142-33154.	1.6	26
118	Cryptochrome 3 from Arabidopsis thaliana: Structural and Functional Analysis of its Complex with a Folate Light Antenna. Journal of Molecular Biology, 2007, 366, 954-964.	2.0	74
119	Mechanistic and Structural Basis of Stereospecific Cβ-Hydroxylation in Calcium-Dependent Antibiotic, a Daptomycin-Type Lipopeptide. ACS Chemical Biology, 2007, 2, 187-196.	1.6	107
120	The β-propeller domain of the trilobed protease fromPyrococcus furiosusreveals an open Velcro topology. Acta Crystallographica Section D: Biological Crystallography, 2007, 63, 179-187.	2.5	7
121	Structural and Functional Insights into a Peptide Bond-Forming Bidomain from a Nonribosomal Peptide Synthetase. Structure, 2007, 15, 781-792.	1.6	152
122	Expression screening of integral membrane proteins from <i>Helicobacter pylori</i> 26695. Protein Science, 2007, 16, 2667-2676.	3.1	13
123	Morphology of Dry Solid-Supported Protein Monolayers Dependent on the Substrate and Protein Surface Properties. Langmuir, 2006, 22, 7185-7191.	1.6	3
124	The Thioesterase Domain of the Fengycin Biosynthesis Cluster: A Structural Base for the Macrocyclization of a Non-ribosomal Lipopeptide. Journal of Molecular Biology, 2006, 359, 876-889.	2.0	110
125	Absorption and fluorescence spectroscopic characterization of cryptochrome 3 from Arabidopsis thaliana. Journal of Photochemistry and Photobiology B: Biology, 2006, 85, 1-16.	1.7	63
126	Light-driven DNA repair by photolyases. Cellular and Molecular Life Sciences, 2006, 63, 1266-1277.	2.4	169

#	Article	IF	CITATIONS
127	Photolyases and cryptochromes: common mechanisms of DNA repair and light-driven signaling?. Current Opinion in Structural Biology, 2006, 16, 51-59.	2.6	62
128	Natural and Non-natural Antenna Chromophores in the DNA Photolyase from Thermus Thermophilus. ChemBioChem, 2006, 7, 1798-1806.	1.3	48
129	Crystallization and preliminary X-ray analysis of cryptochrome 3 fromArabidopsis thaliana. Acta Crystallographica Section F: Structural Biology Communications, 2005, 61, 935-938.	0.7	22
130	Crystal Structure of a Photolyase Bound to a CPD-Like DNA Lesion After in Situ Repair. Science, 2004, 306, 1789-1793.	6.0	350
131	Iron-oxo clusters biomineralizing on protein surfaces: Structural analysis of Halobacterium salinarum DpsA in its low- and high-iron states. Proceedings of the National Academy of Sciences of the United States of America, 2004, 101, 13780-13785.	3.3	111
132	TbPDE1, a novel class I phosphodiesterase of Trypanosoma brucei. FEBS Journal, 2004, 271, 637-647.	0.2	29
133	Structure-Based Mutational Analysis of the 4â€~-Phosphopantetheinyl Transferases Sfp from Bacillus subtilis:  Carrier Protein Recognition and Reaction Mechanism,. Biochemistry, 2004, 43, 4128-4136.	1.2	62
134	Crystal Structure of Halophilic Dodecin. Structure, 2003, 11, 375-385.	1.6	86
135	1.3â€Ã X-ray structure of an antibody Fv fragment used for induced membrane-protein crystallization. Acta Crystallographica Section D: Biological Crystallography, 2003, 59, 677-687.	2.5	4
136	Halorhodopsin: light-driven ion pumping made simple?. Current Opinion in Structural Biology, 2002, 12, 516-522.	2.6	110
137	Structural genomics of "non-standard―proteins: a chance for membrane proteins?. Gene Function & Disease, 2002, 3, 39-48.	0.3	12
138	Crystal structure of the catalytic core component of the alkylhydroperoxide reductase AhpF from Escherichia coli. Journal of Molecular Biology, 2001, 307, 1-8.	2.0	20
139	Purification, Crystallization, and Preliminary X-ray Diffraction Analysis of the Tricorn Protease Hexamer from Thermoplasma acidophilum. Journal of Structural Biology, 2001, 134, 83-87.	1.3	5
140	G-Protein-Coupled Receptors for Light: The Three-Dimensional Structure of Rhodopsin. ChemBioChem, 2001, 2, 513-516.	1.3	3
141	Structural analysis of adenylate cyclases from Trypanosoma brucei in their monomeric state. EMBO Journal, 2001, 20, 433-445.	3.5	56
142	Crystallization and preliminary X-ray analysis of the catalytic domain of the adenylate cyclase GRESAG4.1 fromTrypanosoma brucei. Acta Crystallographica Section D: Biological Crystallography, 2000, 56, 359-362.	2.5	4
143	Crystallization and preliminary X-ray analysis of the catalytic core of the alkylhydroperoxide reductase component AhpF from Escherichia coli. Acta Crystallographica Section D: Biological Crystallography, 2000, 56, 92-94.	2.5	3
144	Crystal structure of the Î ² -apical domain of the thermosome reveals structural plasticity in the protrusion region 1 1Edited by D. Rees. Journal of Molecular Biology, 2000, 301, 19-25.	2.0	23

#	Article	IF	CITATIONS
145	Structure of the Light-Driven Chloride Pump Halorhodopsin at 1.8 Å Resolution. Science, 2000, 288, 1390-1396.	6.0	534
146	Group II chaperonins: new TRiC(k)s and turns of a protein folding machine. Journal of Molecular Biology, 1999, 293, 295-312.	2.0	191
147	A cold break for photoreceptors. Nature, 1998, 392, 131-133.	13.7	9
148	Group II chaperonin in an open conformation examined by electron tomography. Nature Structural Biology, 1998, 5, 855-857.	9.7	100
149	Structural and mechanistic comparison of prokaryotic and eukaryotic phosphoinositide-specific phospholipases C 1 1Edited by K. Nagai. Journal of Molecular Biology, 1998, 275, 635-650.	2.0	121
150	Structural Analysis of the Catalysis and Membrane Association of PLC-δ1. ACS Symposium Series, 1998, , 121-136.	0.5	1
151	Lipid patches in membrane protein oligomers: Crystal structure of the bacteriorhodopsin-lipid complex. Proceedings of the National Academy of Sciences of the United States of America, 1998, 95, 11673-11678.	3.3	429
152	A Ternary Metal Binding Site in the C2 Domain of Phosphoinositide-Specific Phospholipase C-δ1,. Biochemistry, 1997, 36, 2753-2762.	1.2	150
153	Structural Mapping of the Catalytic Mechanism for a Mammalian Phosphoinositide-Specific Phospholipase Câ€,‡. Biochemistry, 1997, 36, 1704-1718.	1.2	122
154	Structure of the Substrate Binding Domain of the Thermosome, an Archaeal Group II Chaperonin. Cell, 1997, 91, 263-270.	13.5	152
155	Crystal Structure of the Bifunctional Soybean Bowman-Birk Inhibitor at 0.28-nm Resolution. Structural Peculiarities in a Folded Protein Conformation. FEBS Journal, 1996, 242, 122-131.	0.2	92
156	C2 domain conformational changes in phospholipase C-δ1. Nature Structural and Molecular Biology, 1996, 3, 788-795.	3.6	113
157	Crystal structure of a mammalian phosphoinositide-specific phospholipase Cδ. Nature, 1996, 380, 595-602.	13.7	591
158	Crystals of an antibody FV fragment against an integral membrane protein diffracting to 1.28 Ã resolution. Proteins: Structure, Function and Bioinformatics, 1995, 21, 74-77.	1.5	22
159	The de Novo Design of an Antibody Combining Site. Journal of Molecular Biology, 1994, 238, 226-244.	2.0	45
160	Single-step purification of a bacterially expressed antibody Fv fragment by immobilized metal affinity chromatography in the presence of betaine. Journal of Chromatography A, 1993, 657, 55-61.	1.8	29
161	Production and secretion in CHO cells of the extracellular domain of AMOGβ2, a type-II membrane protein. Gene, 1992, 120, 307-312.	1.0	12